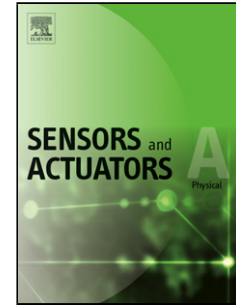


Accepted Manuscript

Title: Design guidelines of Laser Reduced Graphene Oxide Conformal Thermistor for IoT applications

Authors: Francisco J. Romero, Almudena Rinadeneyra, Victor Toral, Encarnación Castillo, Francisco García-Ruiz, Diego P. Morales, Noel Rodríguez



PII: S0924-4247(18)30213-9
DOI: <https://doi.org/10.1016/j.sna.2018.03.014>
Reference: SNA 10680

To appear in: *Sensors and Actuators A*

Received date: 4-2-2018
Revised date: 8-3-2018
Accepted date: 12-3-2018

Please cite this article as: Romero FJ, Rinadeneyra A, Toral V, Castillo E, García-Ruiz F, Morales DP, Rodríguez N, Design guidelines of Laser Reduced Graphene Oxide Conformal Thermistor for IoT applications, *Sensors and Actuators: A Physical* (2010), <https://doi.org/10.1016/j.sna.2018.03.014>

This is a PDF file of an unedited manuscript that has been accepted for publication. As a service to our customers we are providing this early version of the manuscript. The manuscript will undergo copyediting, typesetting, and review of the resulting proof before it is published in its final form. Please note that during the production process errors may be discovered which could affect the content, and all legal disclaimers that apply to the journal pertain.

Design guidelines of Laser Reduced Graphene Oxide Conformal Thermistor for IoT applications

Francisco J. Romero^{1,3,*}, Almudena Rinadeneyra⁴, Victor Toral^{2,3}, Encarnación Castillo^{2,3}, Francisco García-Ruiz^{1,3}, Diego P. Morales^{2,3}, Noel Rodríguez^{1,3}

¹Pervasive Electronics Advanced Research Laboratory. University of Granada

²Electronic Devices Research Group. University of Granada

³Department of Electronics and Computer Technology. University of Granada, Granada 18072, Spain

⁴Technische Universität München, Munich 80333, Germany

*Corresponding author

Highlights

- A flexible laser-lithographed reduced-graphene thermistor is proposed in this paper.
- An IoT sensing system to monitor the ambient temperature in real-time is presented.
- The conditioning electronics is fully based on a reconfigurable platform.

Abstract

This work presents a complete temperature sensing solution based on a conformal laser-reduced graphene-oxide temperature transducer acting as thermistor. The process to implement the temperature-sensitive element is described in detail; from the raw material to the optimum laser scribing conditions used to define the resistive component. The final transducer is fabricated on a flexible plastic substrate and can be attached to any surface as a conformal patch. To provide a full demonstrator of the potential of this technology, the thermistor is integrated in an IoT sensing platform with wireless data transmission capability using a reconfigurable ultra-low power System-on-Chip.

Keywords

Graphene, reduced-Graphene-Oxide, rGO, sensors, SoC, thermistor

1. Introduction

Since in 2010 the Nobel Prize was awarded to A. Geim and K. Novoselov “for the groundbreaking experiments regarding the two-dimensional material”, graphene has become one of the most studied materials in all the fields of technology [1]. Its unique properties combining outstanding electrical conductivity, transparency, toughness and biochemical functionalization capabilities have exponentially attracted the interest of not only fundamental research fields, such as Physics or Chemistry, but also more applied lines, like energy storage or transducers [2]. However, despite graphene’s potential is undeniable, the actual end-user applications are still far from achieving the aroused expectations, mostly due to the difficulties associated with the mass production of high quality graphene sheets capable of matching its theoretical properties.

The broad spectrum of production approaches has opened the term graphene to a set of materials including not only the ideal sp^2 honeycomb and monoatomic carbon structure, but also multilayer polycrystalline graphene aggregates. One of these graphene-like materials is the so called reduced-graphene-oxide (rGO) [3]. Notwithstanding that rGO does not feature the superlative properties of monolayer crystalline graphene, it capitalizes part of its unique features (e.g. flexibility, electrical and thermal conductivity), with the great advantage of a much easier and technologically simpler synthesis process. In addition, rGO’s conductivity presents a very linear dependence with temperature above 200 K as a consequence of its polycrystalline structure [4]. This latter physical characteristic is exploited in this work to develop a temperature transducer (thermistor), taking advantage of the pliancy and low thermal inertia of the rGO [5] and incorporating an application oriented photo-thermal reduction technique [6]. Some of these properties, such as its ductility, make this kind of sensors a pertinent choice for Internet of Things (IoT) applications or even healthcare implantable systems. In this way, the use of graphene or graphene-like based sensors and devices aims to facilitate the interconnectivity that the future Internet of Everything (IoE) environment will need, such as flexible and pervasive devices that shrink the power consumption and enable faster data transmission [7]. In this context, this work presents as a final outcome, a full custom wearable temperature measurement system that illustrates the advantages that this technology brings up to the IoT ecosystem.

The manuscript is divided in five parts. After this introduction, Section 2 introduces the production of rGO from the raw GO colloid. Section 3 provides guidelines for the design of the transducers based on the laser assisted photothermal lithography, and results from their electrothermal characterization. Section 4 describes a complete sensor application adopting the rGO transducer in an ultra-low power platform based on Cypress® 5LP System-on-Chip (SoC). Finally, the main conclusions are drawn in Section 5.

2. Laser Scribing of reduced-Graphene Oxide

The starting point for the proposed rGO-based thermistors is the production of the raw material: the Graphene Oxide colloid (GOc). The GOc is synthesized by oxidation and sonic exfoliation of graphite powder. In our samples, we follow a modified version of Hummers and Offerman method [8], schematized in Figure 1. For about two hours Graphite is oxidized, in an ice bath, using strong oxidizing reagents like concentrated

sulfuric acid (H_2SO_4); sodium nitrate (NaNO_3); and potassium permanganate (KMnO_4). The temperature should be maintained low to avoid any risk of explosion (Figure 1, ice bath). Compared to pristine graphite, GO is strongly oxygenated through functional hydroxyl ($-\text{OH}$) and epoxide ($\text{C}-\text{O}-\text{C}$) groups in the basal plane of the atoms with sp^3 sp^2 hybridized planes [9]. After the oxidation, the graphite is filtered (HCl) and washed (H_2O) to remove remaining ions. Then, the hydrophilic nature of GO and the increased interlayer distance caused by the introduction of the functional groups permits easy penetration of water molecules, allowing layer splitting through sonication (or continuous stirring) in water dispersion. We sonicated the dispersion (4mg mL^{-1}) for 30 minutes taking care of keeping the temperature low enough to avoid the thermal reduction of the GO. Surface charges on the GO are highly negative when dispersed in water due to the carboxylic acid ionization and phenolic-hydroxyl groups. This leads to an electrostatic repulsion that avoids the aggregation of the GOc [3].

The GOc can be deposited as a thin and uniform film (spin-coated, vortex shaker...) on any non-porous surface (structurally flexible or not) and turned into rGO through a reduction process. GO is an electrical insulator due to the disruption of the crystallographic network of carbon atoms during the oxidation process. However, the electrical conductivity is restored during the reduction by the removal of the functional groups and the partial healing of the crystallographic structure [10]. Among all the existing reduction procedures, we selected the laser photothermal reduction [6] as the best alternative since: *i*) it is environmental friendly, *ii*) it allows precise patterning of conductive elements without the use of hard masks, and *iii*) the conductivity of the resulting rGO can be modulated by the laser photothermal power.

As confirmed by Raman spectroscopy, the 550 nm (up to 300 mW) laser used in this work is able to reduce effectively the GO. The reduction process manifests itself through the change in the intensity ratio of the two main peaks: D and G located at 1352 cm^{-1} and 1600 cm^{-1} , respectively. The G peak is related to the relative movement of sp^2 pairs of atoms, whereas the D peak is associated to distortions in the structure [11]. The 2D peak (2700 cm^{-1}) is the result of a second order resonant process. In general, the larger the ratio between the 2D and D peaks, the better the quality of the graphene sample obtained [12]. In Figure 2, the 2D peak is almost non-existent before the photothermal treatment. But once the laser healing is applied, the 2D peak rises with a large intensity as a consequence of the restoration of the crystallographic structure and the reduction of the number of defects.

We studied the dependence of the sheet resistance of the laser-rGO as a function of the photothermal power and the initial concentration of GO deposited on the surface before the reduction process. The measurements were conducted by means of four-point-contact kelvin method [13]. Results summarized in Figure 3 show that, independently of the GO concentration, the increase of the photothermal power decreases dramatically the sheet resistance of the sample, ranging from over-M Ω /sq to sub-k Ω /sq values in a relatively narrow power window. Nevertheless, we observed that the decrease in the sheet resistance tends to saturate for a photothermal power above 90 mW. Any further increase in the laser power does not benefit the conductivity but rather it can compromise the integrity of the substrate, especially on flexible organic substrates (PET in this case). The initial concentration of the GO before the reduction plays also a role in

the resultant conductivity obtained. According to our measurements, the lower the concentration, the better the conductivity obtained, with saturation above $90 \mu\text{g cm}^{-2}$. Below $50 \mu\text{g cm}^{-2}$, it is more difficult to control the homogeneity of the deposited GO, leading to non-conductive areas. For concentrations above $150 \mu\text{g cm}^{-2}$, the increase in the sheet resistance (decrease in conductivity after the reduction) also tends to saturate since, only the surface of the deposited GO is effectively reduced, whereas the layers beneath remain unreduced (confirmed by *Scotch* tape exfoliation).

In order to achieve the utmost reliability and simultaneously, to minimize variability of the manufactured thermistor prototypes, we tried to mitigate the effect of the synthesis variables, controlling the total resistance of the transductive element only from its physical dimensions. To do so, we set the photothermal power to 100 mW (where any shift of the power has minor effect according to Figure 3 and the integrity of the substrate is guaranteed in terms of local heat dissipation) and the concentration of GO to $70 \mu\text{gcm}^{-2}$ (where the conductivity of the laser-rGO is very stable).

3. Design of rGO thermal transducers

The conductivity of single GO/rGO flakes has been already studied in detail [14]; however, the number of works which exploit the conduction mechanism in large deposited polycrystalline films of rGO is more reduced. In this regard, we have focused our attention on studying the behavior of the conductivity with respect to temperature, rather than analyzing the ultimate physical mechanisms responsible for its conduction. The design of the transducer is dimension-based being its total resistance (R) determined by the sheet resistance of the laser-rGO (ρ_s), width (W) and length (L) of the patterned resistive element ($R_T = \rho_s L/W$). For our prototypes (Figure 4 inset), the access to the transducer is implemented by thin copper electrodes. The contact surface between the rGO and copper is coated with conductive silver ink (Merck Dyesol® DYAG350) to decrease the contact resistance and ensure permanent electrical connection. The contact resistance obtained using this method is between 100Ω and 150Ω , having no impact if the transducers are designed for a nominal resistance over the $\text{k}\Omega$ range. Once the GO is deposited on the polyethylene terephthalate (PET) film, laser-reduced, patterned and contacted, the exposed surface is vacuum sealed with another PET film to prevent direct contact with the atmosphere. This is done to avoid the progressive passivation of the functional groups remaining on the GO surface by the capture of molecules that may cause a slight time drift on the nominal resistance.

Figure 4 depicts the calibration curve of one of the developed prototypes ($L = 25 \text{ cm}$, $W = 0.5 \text{ cm}$). The transducer has been heated and cooled with the aid of a climate chamber (Vötsch, Model VCL 4003) at two Relative Humidity levels ($RH = 0\%$ and $RH = 50\%$) while the temperature was being monitored. As observed, the resistance shows a perfectly linear dependence with temperature, facilitating the definition of a calibration curve. However it is worth to mention that this linear law, with RH independence, can only be obtained when the transducer is fully sealed. As shown in Figure 4, the transducer resistance ranges between $[140, 100] \text{ k}\Omega$ inside the temperature window

[243, 308] K. This resistance can be adjusted by changing the photothermal lithography pattern. The absolute sensitivity for this example geometry (Figure 4 inset) is $-599.3 \text{ } \Omega/\text{K}$, which yields a relative sensitivity $[(\Delta R/R_{273\text{K}})/(T - 273\text{K}) = ((R - R_{273\text{K}})/R_{273\text{K}})/(T - 273\text{K})]$ of $0.489 \text{ } \%/ \text{K}$ in the range of temperature studied (243-308 K). It is worth mentioning that this value is virtually independent of the rGO lithographed pattern. Only for very long serpentine patterns we corroborated a fluctuation in the sensitivity (up to 0.12%) attributed to an increase/decrease of the physical dimensions of the transducer with the temperature change.

The resultant sensitivity is similar to the obtained with other not graphene-based flexible temperature sensors whose synthesis process is technologically more complex [15][16]. Inside the field of the graphene research applications, Sahoo et al. [17] also presented a rGO-based transducer, reduced on an Al_2O_3 substrate, with a sensitivity of $0.195 \text{ } \%/ \text{K}$, about half of the obtained with the photothermal reduction. Another example of a flexible temperature sensor based on graphene is the presented by Zhao et al. [18]. In this case, a brush mess was used for the Chemical Vapor Deposition (CVD) growth of Graphene Woven Fabrics (GWFs) and transferred afterwards onto a PET substrate, obtaining a sensitivity almost three times higher than the presented in this work. However, this method is significantly less cost-effective for the mass production of transducers. As summary, Table 1 presents a comparison between the transducer sensitivity presented in this work and others graphene-based as well as non-graphene-based flexible temperature sensors.

Two aspects should be considered regarding the operation range of these rGO-based transducers. On one hand, if the transducer is laser lithographed maintaining unreduced areas (like in the serpentine pattern), those regions could be progressively reduced if the sensor is maintained at high temperature. The ratio of reduction depends on the temperature and time, but as a general rule to avoid resistance drift, the sensor should be kept below 400 K . This is not a limitation for a fully reduced surface (like a rectangle). On the other hand, at very low temperature ($< 200 \text{ K}$) (not tested here), the characteristic may become non-linear, requiring a more sophisticated calibration law [4].

Finally, the impedance of a prototype transducer has been analyzed as a function of frequency. Results evidence a purely resistive behavior up to the 10 kHz of excitation frequency (see Figure 5), ensuring in this way a fast electrical response. Well beyond 10 kHz , the phase of the impedance turns negative, displaying a parasitic parallel capacitive contribution ($Z_T = R_T / (1 + j 2\pi f R_T C)$). From the results in Figure 5, the parasitic capacitance of the transducer can be considered very low ($\sim 95 \text{ pF}$ for this particular case), ensuring a very fast electrical response.

4. Ultra-Low Power sensor application

The use of any temperature sensor prototype is intimately related to the design of the conditioning interface that provides its information to the final user. Furthermore, in the IoT era [20], the electronic instrumentation designed for an emerging sensor prototype must underline the advantages of this technology and envision the myriads of

environments where this device could be employed, especially enhancing the sensor-instrumentation symbiosis inside the IoT context. The main characteristics of an IoT sensor system can be sum up as small size, low-power consumption and the communication capability with the sensor environment [21]. With these skills, the sensor device can be integrated in quite a lot of different systems. In general terms of analog sensors, the design of an instrumentation interface for a sensor node must cope with far different scenarios because of the inherent variability in the output from one to another physical sensor prototype. For this reason, the use of reconfigurable electronic systems is a powerful solution. This alternative might seem unsuitable and uncompetitive for a commercial final version, but the recent advances in the development of programmable SoC for IoT applications [22] with reconfigurable skills, in both digital and analog domains, make this choice as powerful as the full-custom designs [23]. In addition, the solutions based on SoCs help to reduce the time-to-market and also making easier the design of sensor-based systems due to their programmable Analog Front Ends (AFE). Previous works show the versatility of this approach for sensor instrumentation applications [24-26].

The developed prototype uses the Programmable SoC (PSoC) model V from Cypress®, in particular the low-power version [27]. The PSoC 5LP offers numerous advantages over the older versions, specifically in terms of performance, quality and low-power operation, being ideal for IoT applications. The philosophy of this approach is to ensure that all the analog and digital resources that could be necessary for an IoT sensor design are in the same silicon die. This enables the design of a miniaturized sensor system that can be attached or integrated in almost any object, such as wearables or even implantable medical devices.

The prototype, shown in Figure 6, has been developed to measure the ambient temperature using the rGO thermal transducer previously described. Then, this temperature is sent by Bluetooth Low Energy (BLE, or Bluetooth 4.0) to a master device, e.g., a smartphone. Therefore, a BLE module based on the CC2541 [28] is used for the data transmission in addition to the PSoC 5LP.

For rGO thermistors, the resistance decreases lineally as the temperature rises in the studied temperature range (Figure 4). In this case, and in order to alleviate the voltage reference dependencies, a ratiometric resistor divider method has been implemented to measure the thermistor resistance. As detailed before, the fact of using a PSoC-based device reduces the signal conditioning complexity since only one external reference resistor is needed. The value of the selected R_{REF} should be as similar as possible to the thermistor resistance at the central value of temperature in the range considered to take advantage of both temperature and Analog-to-Digital Converter (ADC) dynamic range.

The full hardware configuration of the PSoC is shown in Figure 7. This design has been implemented using the PSoC Creator Integrated Design Environment (IDE), which makes possible the design of concurrent hardware and application firmware. As seen in Figure 7, the simplest way to supply power the external circuit would be using the voltage of the battery as V_{HI} , which would also reduce the resolution required for the ADC. However, for ultra-low power consumption, the current through the resistor divider must be as low as possible. In this way, there should be a compromise between

V_{HI} (responsible of the current across the resistors) and the resolution of the ADC (temperature resolution). Besides, a Voltage Digital-to-Analog Converter (VDAC) helps limiting the current consumption thanks to the resistor divider since it can be turned on only when a measurement is taken. The PSoC pin used to measure V_{THERM} must be set to High-Z to avoid current leakages. This configuration, together with the variation ΔR_T in the range of interest, delivers a temperature resolution of ± 0.001 K.

Once the temperature is measured, the device developed performs a peripheral role with respect to the BLE communication. A full-duplex Universal Asynchronous Receiver-Transmitter (UART) module, which is the interface with the BLE module, works as a slave of a central/master device. Due to the standardization of the Bluetooth 4.0 services, any device that incorporates this kind of communication protocol could serve as the master device. In this work, a smartphone has been chosen to widen its potential use.

One of the critical issues in instrumentation is the power efficiency, directly related with the battery lifetime. The consumption of the presented prototype is mainly associated to the software execution, and hence to the SoC hardware peripherals involved on it. The program execution cycle must be optimized to reduce the power consumption. SoCs offer the possibility of turning off its peripherals when are not being used, which implies a substantial energy saving without compromising its functionality. In this case, the sensor device is in idle state until a timer timeout triggers the process to carry out a measurement, then the VDAC is turned on only the time required for an ADC single-shot conversion. Once the temperature is computed and sent, the device returns back to low-power mode (idle).

The power supply can be provided by an external battery or by a MicroUSB connector depending on the specific application. However, most ultra-low power sensor applications require the use of batteries. Therefore, it is also important to estimate in advance the battery life-time, which depends on the frequency of the measurement. For example, in a room temperature monitoring application which measures the temperature every five minutes, the average current of this device is assessed to be below $10 \mu\text{A}$ (sensor current included). Thus, the estimation of the battery life-time would be, using the most common coin cell battery (CR2032), of about 2 years.

As an illustrative example of end user application, we present a car outdoor thermometer (Figure 9). The transducer was attached, as a conformal patch, to the right rear-view mirror of the car, and the wireless device was located inside it to monitor the ambient temperature. The graph inset in Figure 9 presents the recorded temperature during 24 hours.

Finally, we advocate that once the SoC systems become available on flexible substrates, rGO-based sensors will take a big step forward expanding to multiple ubiquitous applications. For example, the combination of this technology, which is compatible with the human tissue, with self-powered or passively-powered microcontrollers and transceivers would make the medical implants smarter, more accurate, human-friendly and inexpensive.

5. Conclusions

Graphene Oxide has been suited as a sensing platform ready to be exported to certain end-user applications. We have presented a prototype of temperature monitoring solution, covering aspects from the production of the raw material to the design and integration on a SoC. Once the GO is deposited on the supporting substrate, a simple process is followed to create the transducer: a CNC-laser scribes the desired pattern, yielding a conductivity that can be easily predicted and controlled by the dimensional aspects of the pattern as well as the concentration of GO and laser photothermal power. The final transducer is fabricated on a flexible PET substrate and can be attached to any surface as a conformal patch throwing a very competitive sensitivity when compared with other flexible transducers at a lower production cost. The final complete wireless SoC-based sensing solution presented constitutes an actual demonstrator of the potential of the GO for the implementation of versatile and flexible substrates-friendly sensing solutions.

Acknowledgements

Thanks are due to the Center of Scientific Instrumentation of the University of Granada (CIC-UGR) for Raman Spectroscopy experiments.

This work has been partially supported by the Spanish Ministry of Education, Culture and Sport (MECD), the European Union and the University of Granada through the project TEC2017-89955-P, the pre-doctoral grant FPU16/01451, the fellowship H2020-MSCA-IF-2017 794885-SELFSENS and the grant “Initiation to Research”.

The authors would like to thank Prof. A. Palma for the climate chamber support.

References

- [1] A.K. Geim, K.S. Novoselov, *The rise of graphene*, Nature materials, 6(2007) 183-191.
- [2] B. Vargas-Quesada, Z. Chinchilla-Rodríguez, N. Rodríguez, *Identification and Visualization of the intellectual structure in graphene research*, Frontiers in Research Metrics and Analytics, 2(2017) 7.
- [3] A.M. Dimiev, S. Eigler, *Graphene oxide: Fundamentals and applications*, John Wiley & Sons, (2016).
- [4] E.P. Neustroev, M.V. Nogovitsyna, Y.S. Solovyova, G.N. Alexandrov, E.K. Burtseva, *Study of electrical conductivity of thermally reduced graphene oxide*, RENSIT Nanosystems, 7(2015) 162-167.
- [5] S. Sahoo, S.K. Barik, G.L. Sharma, G. Khurana, J.F. Scott, R.S. Katiyar, *Chemically prepared reduced graphene oxide as ultra fast temperature sensor*, The Electrochemical Society Meeting, (2012).
- [6] E. Kymakis, C. Petridis, T.D. Anthopoulos, E. Stratakis, *Laser-assisted reduction of graphene oxide for flexible, large-area optoelectronics*, IEEE Journal of Selected Topics in Quantum Electronics, 20(2014) 106-115.
- [7] E. Alahi, A. Nag, S. C. Mukhopadhyay, L. Burkitt, *A temperature-compensated graphene sensor for nitrate monitoring in real-time application*, Sensors and Actuators A, 269(2018) 79–90.
- [8] W.S. Hummers Jr, R.E. Offeman, *Preparation of graphitic oxide*, Journal of the American Chemical Society, 80(1958) 1339-1339.
- [9] D.R. Dreyer, S. Park, C.W. Bielawski, R.S. Ruoff, *The chemistry of graphene oxide*, Chemical Society Reviews, 39(2010) 228-240.

- [10] S. Pei, H.-M. Cheng, *The reduction of graphene oxide*, Carbon, 50(2012) 3210-3228.
- [11] F. Tuinstra, J.L. Koenig, *Raman spectrum of graphite*, The Journal of Chemical Physics, 53(1970) 1126-1130.
- [12] A.C. Ferrari, J. Meyer, V. Scardaci, C. Casiraghi, M. Lazzeri, F. Mauri, et al., *Raman spectrum of graphene and graphene layers*, Physical review letters, 97(2006) 187401.
- [13] D.K. Schroder, *Semiconductor material and device characterization*, John Wiley & Sons, (2006).
- [14] D. Joung, S.I. Khondaker, *Efros-Shklovskii variable-range hopping in reduced graphene oxide sheets of varying carbon sp² fraction*, Physical Review B, 86(2012) 235423.
- [15] S. Harada, W. Honda, T. Arie, S. Akita, K. Takei, *Fully Printed, Highly Sensitive Multifunctional Artificial Electronic Whisker Arrays Integrated with Strain and Temperature Sensors*, ACS Nano, 8(4)(2014) 3921–3927.
- [16] W. Honda, S. Harada, T. Arie, S. Akita, K. Takei, *Wearable, Human-Interactive, Health-Monitoring, Wireless Devices Fabricated by Macroscale Printing Techniques*, Adv. Funct. Mater, 24 (2014) 3299–3304.
- [17] S. Sahoo, S. K. Barik, G. L. Sharma, G. Khurana, J. F. Scott, R. S. Katiyar, *Reduced graphene oxide as ultra-fast temperature sensor*, arXiv (2012).
- [18] X. Zhao, Y. Long, T. Yang, J. Li, H. Zhu, *Simultaneous High Sensitivity Sensing of Temperature and Humidity with Graphene Woven Fabrics*, ACS Appl. Mater. Interfaces, 9(35)(2017) 30171–30176.
- [19] F. Xue, L. Zhang, W. Tang, C. Zhang, W. Du, Z. L. Wang, *Piezotronic Effect on ZnO Nanowire Film Based Temperature Sensor*, ACS Appl. Mater. Interfaces, 6(8)(2014) 5955–5961.
- [20] D. Miorandi, S. Sicari, F. De Pellegrini, I. Chlamtac, *Internet of things: Vision, applications and research challenges*, Ad Hoc Networks, 10(2012) 1497-1516.
- [21] J. Gubbi, R. Buyya, S. Marusic, M. Palaniswami, *Internet of Things (IoT): A vision, architectural elements, and future directions*, Future generation computer systems, 29(2013) 1645-1660.
- [22] R. Aitken, V. Chandra, J. Myers, B. Sandhu, L. Shifren, G. Yeric, *Device and technology implications of the Internet of Things*, VLSI Technology (VLSI-Technology): Digest of Technical Papers, (2014).
- [23] Cypress Semiconductor, “Wearables Solutions Catalog”. [Accessed on: 15/02/2018].
- [24] A. Salinas-Castillo, D.P. Morales, A. Lapresta-Fernández, M. Ariza-Avidad, E. Castillo, A. Martínez-Olmos, et al., *Evaluation of a reconfigurable portable instrument for copper determination based on luminescent carbon dots*, Analytical and bioanalytical chemistry, 408(2016) 3013-3020.
- [25] D. Morales, N. López-Ruiz, E. Castillo, A. García, A. Martínez-Olmos, *Adaptive ECT system based on reconfigurable electronics*, Measurement, 74(2015) 238-245.
- [26] D. Morales, A. Garcia, A. Martínez Olmos, J. Banqueri, A. Palma, *Digital and analog reconfiguration techniques for rapid smart sensor system prototyping*, Sensor Letters, 7(2009) 1113-1118.
- [27] Cypress Semiconductor, “PSoC® 5LP: CY8C52LP Family Datasheet”. [Accessed on: 15/02/2018].
- [28] Texas Instrument, “CC2541, 2.4-GHz Bluetooth™ low energy and Proprietary System-on-Chip”. [Accessed on: 15/02/2018].

[29] Cypress Semiconductor, “PSoC® 3, PSoC 4, and PSoC 5LP Temperature Sensing with a Thermistor”. [Accessed on: 15/02/2018].

Biographies

Francisco J. Romero received the B.Eng. with valedictorian mention in Telecommunications Engineering from the University of Granada (Spain) in 2016. In 2015, he joined the Department of Electronics and Computer Technology at the University of Granada as a Junior Researcher, and in 2017 became a PhD Candidate with a national predoctoral scholarship. His current research interests are related to IoT embedded systems and 2D-materials-based sensors.

Almudena Rivadeneyra completed her master’s degrees in telecommunication engineering (2009), environmental sciences (2009) and electronics engineering (2012), at the University of Granada (Spain). In 2014, she received her PhD in design and development of environmental sensors at the same Institution. Since 2015, she belongs to the Institute for Nanoelectronics (Technical University of Munich) where her work is centered in printed and flexible electronics. She is co-author of more than 40 scientific contributions.

Victor Toral received the B.Eng. in Electronics Engineering from the University of Granada (Spain) in 2017. In 2016, he joined the Department of Electronics and Computer Technology of the University of Granada as a Junior Researcher. He is pursuing a master’s degree in power electronics at the University Polytechnic of Madrid (Spain). His main research interests are related to power electronics and electronic instrumentation.

Encarnación Castillo received the degree in Electronic Engineering and PhD “Summa cum Laude” from the University of Granada (Spain) in 2002 and 2008, respectively. From 2003 to 2005 she has been PhD student and from 2006 she is an Assistant Professor, both at the Department of Electronics and Computer Technology at the University of Granada. As part of the thesis research, she made two short stays during at the FAMU-FSU, College of Engineering in Tallahassee. Her research interests include the protection of IP Core Protection as well as RNS arithmetic, high-performance digital signal processing and VLSI and FPL signal processing systems.

Francisco G. Ruiz received his Telecommunication engineering degree from the University of Málaga in 2002 and his PhD in electromagnetism from the University of Granada in 2005. He has been a visiting researcher at IRCTR - TU Delft, IMEC, UCL (Louvain-la-Neuve) and the Group of Graphene-based Nanotechnology - University of Siegen. He is currently with the Pervasive Electronics Advanced Research Laboratory (PEARL), Department of Electronics, University of Granada. His main research interests are simulation, modeling and characterization of electron devices, in particular 2D-materials-based devices and sensors.

Diego P. Morales received the M.Sc. degree in Electronic Engineering and the PhD degree in Electronic Engineering from the University of Granada (Granada, Spain) in

2001 and 2011, respectively. He was an Associate Professor at the Department of Computer Architecture and Electronics, University of Almería (Almería, Spain) before joining the Department of Electronics and Computer Technology at the University of Granada, where he currently serves as an Associate Professor. His current research is devoted to developing reconfigurable applications.

Noel Rodriguez received the B.Eng. with a first national award and M.Eng. in Electronics Engineering from the University of Granada, Spain, in 2004 and 2006 respectively. In 2008, he received a double Ph.D. from the University of Granada and the Institute National Polytechnique of Grenoble. During his Ph.D., he was awarded a grant inside the EDITH Marie Curie program allowing him to spend one year at the IMEP-Minatec facilities (France) where he worked on electrical characterization techniques. He is currently Tenured Professor at the University of Granada and co-founder of the Pervasive Electronics Advanced Research Laboratory. His research interest includes the development of new technologies for ubiquitous electronics and the simulation, modeling and characterization of memory devices with the emphasis in memristive systems and neuromorphic applications. Dr. Noel Rodriguez is co-holder of 9 patents related to the A-RAM memory technology, and he is author or co-author of 8 book chapters and more than 100 scientific contributions.

Figures

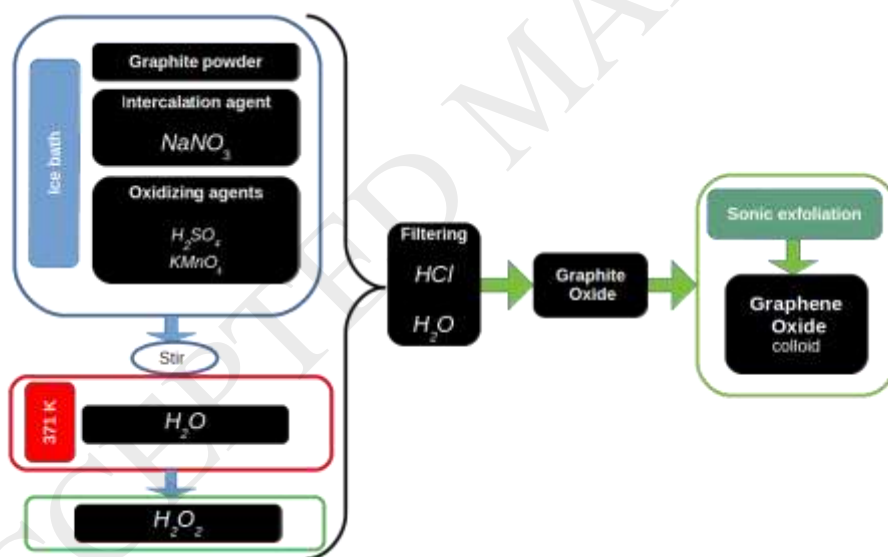


Figure 1. Schematic diagram summarizing the procedure followed to obtain GO.

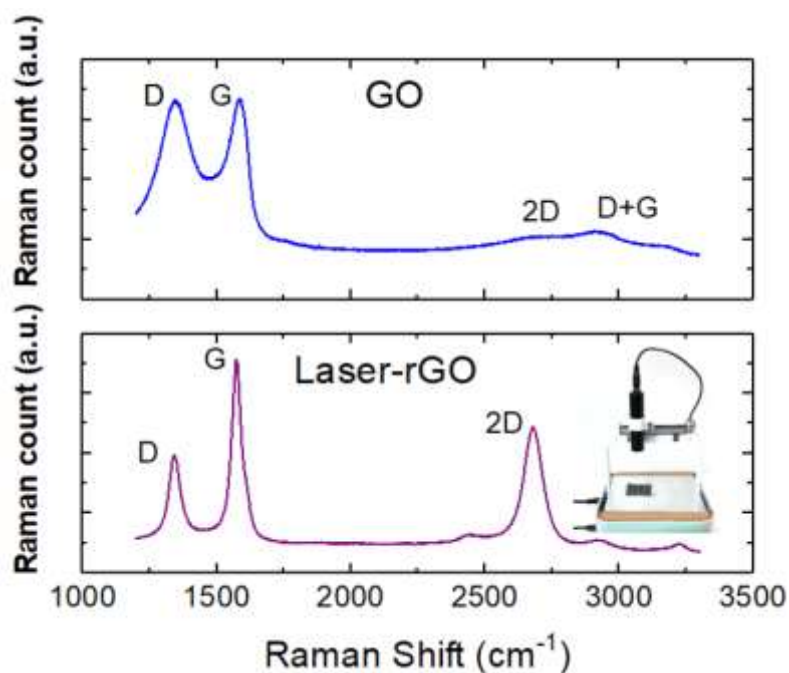


Figure 2. Raman spectra of GO and laser-reduced GO spin-coated on a PET film at a concentration of $400 \mu\text{gcm}^{-2}$. A confocal micro-Raman spectrometer with a 532 nm (green) excitation laser was used. The reduction of GO was achieved by a 550 nm laser, with a photothermal power of 100 mW at an excursion rate of 3 min cm^{-2} and a continuous laser spot. An actual picture of the laser setup is shown at the bottom left-side of the Figure.

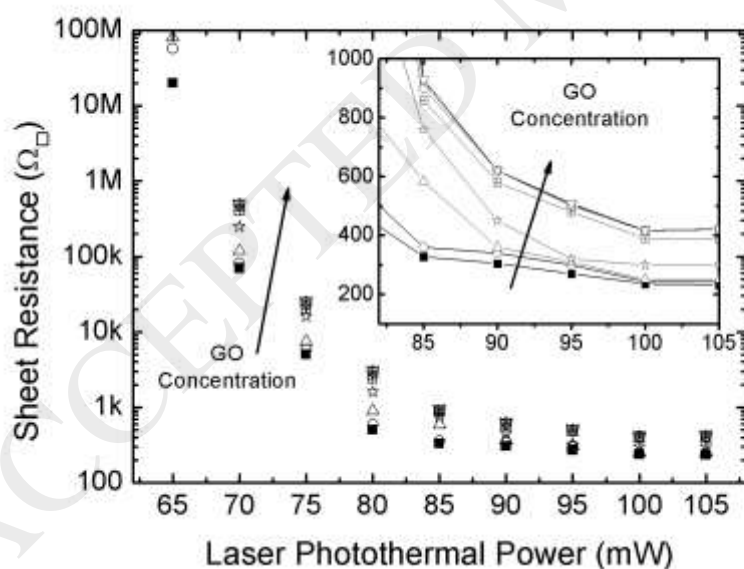


Figure 3. Laser-rGO sheet resistance extracted from kelvin measurements as a function of the laser photothermal power (550 nm laser) for different values of the initial deposited GO ($50, 70, 100, 130, 150, 160, 180, 200 \mu\text{g cm}^{-2}$). Inset shows a magnification in the range of 80 to 105 mW for an excursion rate of 3 min cm^{-2} with a continuous laser spot. Laser power above 120 mW can overheat the PET container substrate.

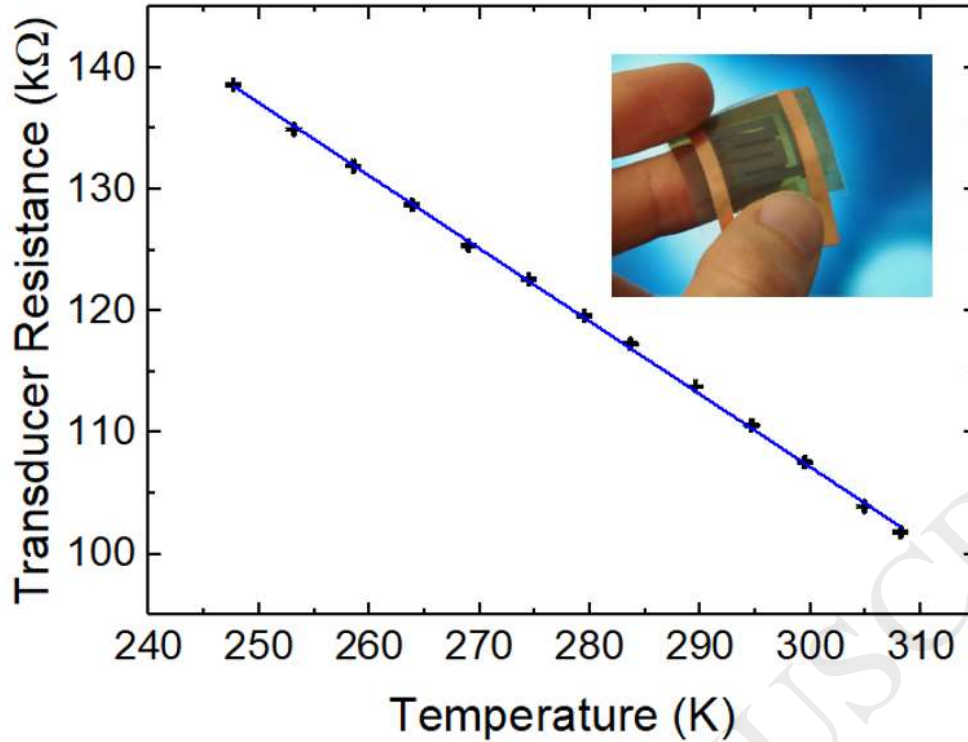


Figure 4. Total resistance of a thermistive transducer fabricated on laser-rGO as a function of temperature. The values of resistance are obtained at RH=0% and RH=50% showing no difference if the transducer is sealed. Inset shows an example of a flexible thermistive transducer sandwiched between two PET films and connected through copper electrodes.

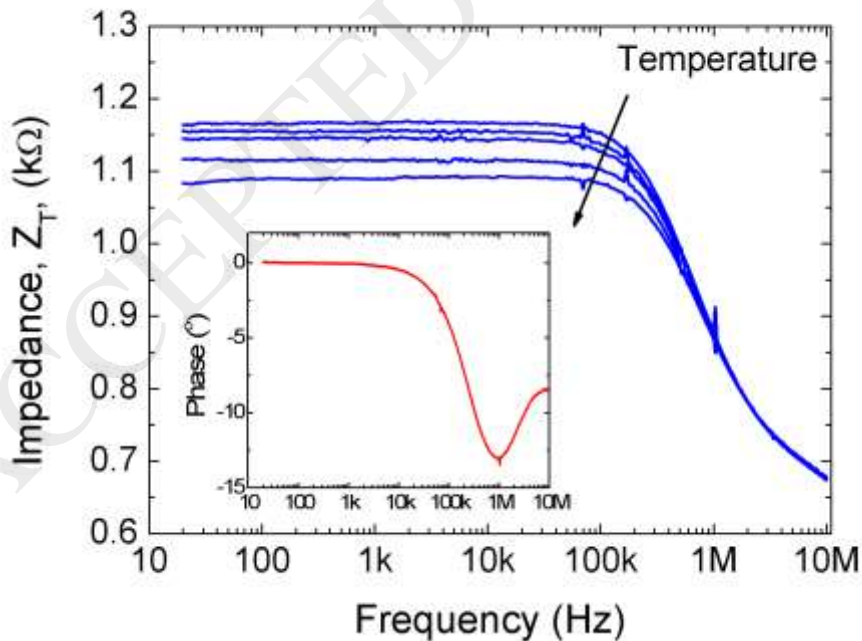


Figure 5. Impedance plot of a rectangular ($L = 2\text{ cm}$, $W = 0.5\text{ cm}$) laser-rGO thermistor. The impedance presents a purely resistive signature even beyond 10 kHz. At high frequency, the phase turns negative reflecting the appearance of a capacitive behaviour.

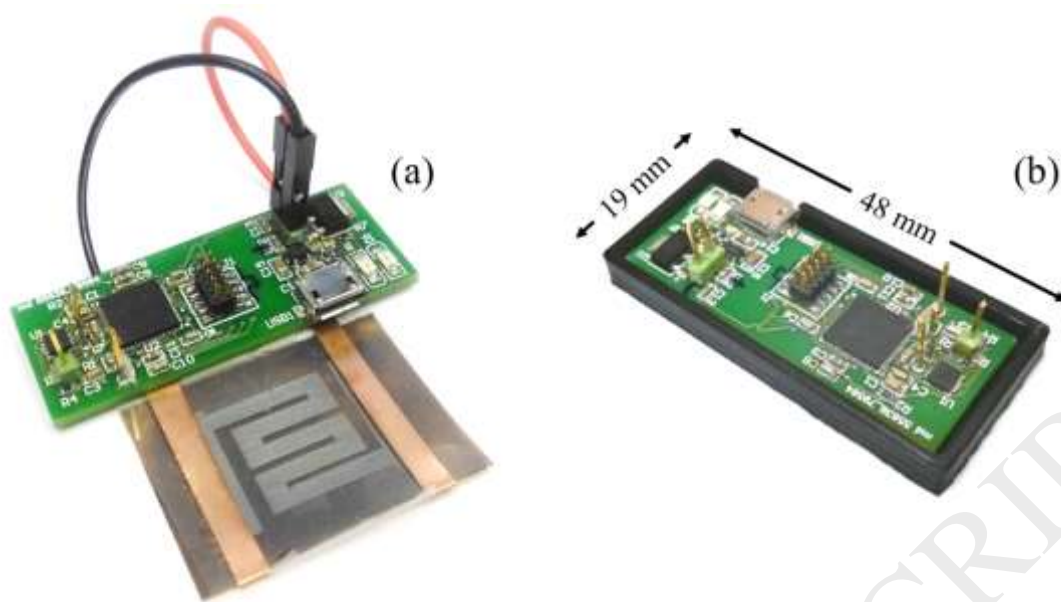


Figure 6. Real view (sensor connected (a), and inside a housing (b)), of the electronic portable device developed for temperature measurements using the laser-rGO thermistor.

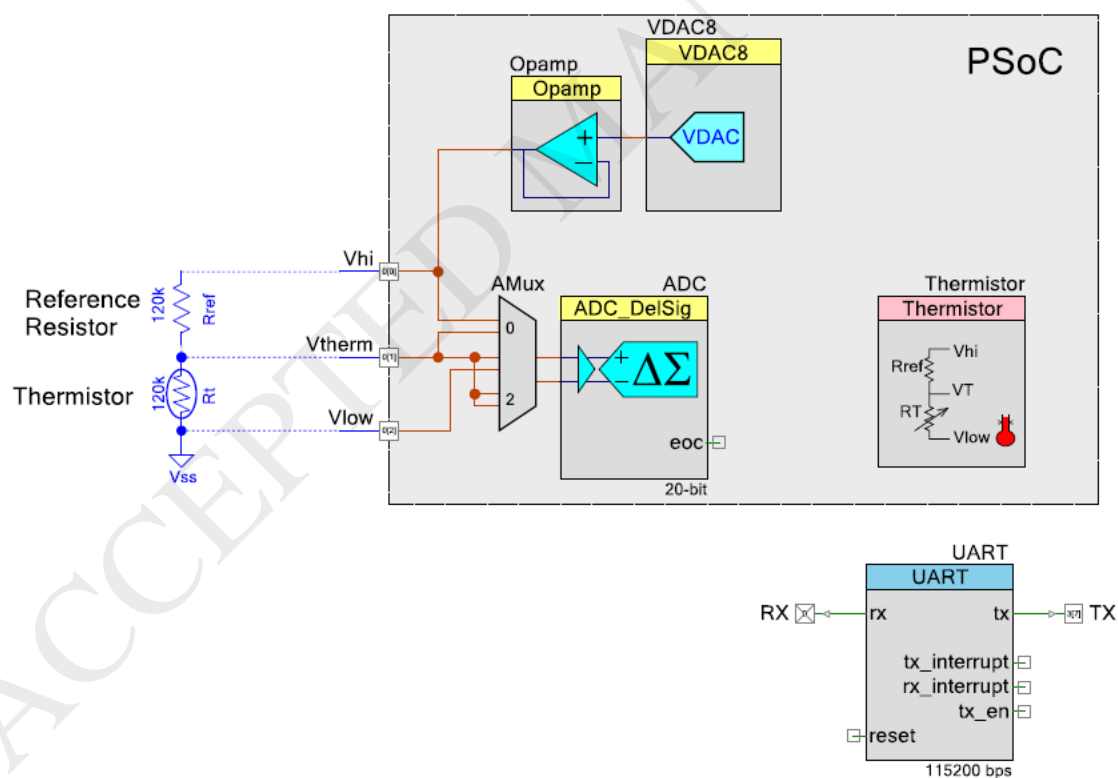


Figure 7. Laser-rGO thermistor measurement circuit for the prototype shown in Figure 6. This design is a custom modification of the project CE210514 from Cypress [29].

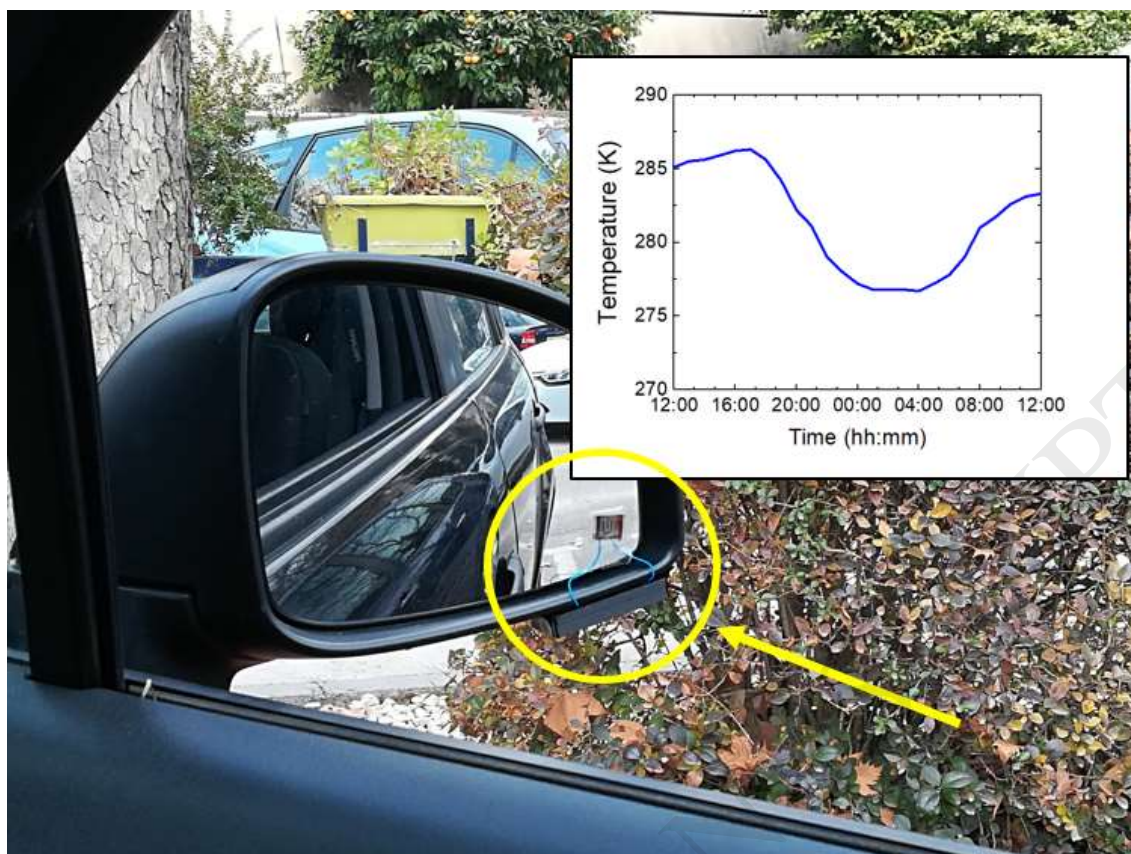


Figure 8. Temperature sensing solution integrated in the side-view mirror of a car. Inset shows the temperature recorded during a whole day.

Table 1. Comparison among close related temperature sensors.

	Zhao et al. [18]	Harada et al. [15]	Honda et al. [16]	Sahoo et al. [17]	Xue et al. [19]	This work
Sensitive layer	GWF	PEDOT:PSS-CNT	PEDOT:PSS-CNT	rGO	ZnO NW	rGO
Substrate	PDMS	PET	Kapton	Al ₂ O ₃	PET	PET
Temperature Range (K)	296 - 328	299 - 326	295 - 326	80 - 375	283 - 383	243 - 308
Sensitivity (%/K)	1.343	0.63	0.61	0.195	[0.98, 3.05]	0.488